Electronic Supplementary Material (ESI) for Nanoscale.

Electronic Supplementary Information:

Self-assembly of a robust hydrogen-bonded octylphosphonate network on cesium lead bromide perovskite nanocrystals for light-emitting diodes

Alasdair A. M. Brown,[a,b,c,d] Thomas J. N. Hooper,[d] Sjoerd A. Veldhuis,[d] Xin Yu Chin,[d] Annalisa Bruno,[d] Parth Vashishtha,[d,e] Ju Nie Tey,[b] Liudi Jiang,[a] Bahulayan Damodaran,[d] Suan Hui Pu,[a,c] Subodh G. Mhaisalkar,[d,e] and Nripan Mathews*[d,e]*

[a]School of Engineering, Faculty of Engineering and Physical Sciences, University of Southampton, Southampton SO17 1BJ, U.K.

[b]Agency for Science and Technology Research (A*STAR) Singapore Institute of Manufacturing Technology (SIMTech), 73 Nanyang Drive, Singapore 637662, Republic of Singapore

[c]University of Southampton Malaysia, Iskandar Puteri 79200, Johor, Malaysia

[d]Energy Research Institute at NTU (ERI@N), Research Techno Plaza, X-Frontier Block Level 5, 50 Nanyang Drive, Singapore 637553, Republic of Singapore

[e]School of Materials Science and Engineering, Nanyang Technological University, 50 Nanyang Avenue, Singapore 639798, Republic of Singapore

CHARACTERISATION METHODOLOGY

Scanning Transmission Electron Microscopy: Measurements were performed with a Tecnai G2 F20 with a Schottky field emitter operated at 200 kV. Selected samples were diluted in toluene, drop-cast on a carbon-copper grid, and mounted on an FEI Double Tilt Analytical Holder for examination. Tecnai G2 F20 STEM with X-Twin objective lenses and field emission gun (Schottky field emitter) operates at a beam current of >100 nA, providing high probe current (0.5 nA or more in 1 nm probe).

Small-Angle X-Ray Scattering (SAXS): Small-angle X-ray scattering (SAXS) measurements were conducted using a Xenocs Nano-inXider, equipped with a Dectris Pilatus3 hybrid pixel detector. This allowed measurement of the effective scattering vector magnitude in the range of $0.0821 < q < 4.47$ nm^{-1} in SAXS. The samples were measured in sealed glass capillaries under vacuum at room temperature. Particle size distributions were obtained (form-free) from scattering curves using the Monte Carlo-based software package McSAS, using a convergence criterion of 5, with 10 calculating repetitions, and 300 contributions.[1]

Optical Absorption Spectroscopy: Absorbance spectra of diluted samples of stably dispersed nanocrystal inks were collected in Quartz cuvettes using a Shimadzu UV-3600 spectrophotometer, from 600 - 350 nm with 0.5 nm steps (0.1 s integration time).

Photoluminescence Spectroscopy: Photoluminescence spectra of diluted sample of stably dispersed nanocrystal inks were collected in Quartz cuvettes using a Horiba Fluoromax-4 spectrophotometer at a laser excitation wavelength of 365 nm (0.1 s integration time, 1 nm/0.5 nm excitation/emission slits). For all spectra, the measured PL intensity was corrected for the absorbance intensity at the excitation wavelength according to: $PL_{corrected} = PL_{measured} / (1-10^{-Abs})$.

Photoluminescence Quantum Yield (PLQY): A 445 nm diode laser (Cobolt) is used to excite the nanocrystal solution. The emission is collected by an integrating sphere (Labsphere) coupled to a monochromator (Andor Kymera), in which the emission intensity is registered by a photomultiplier tube.

Time-Resolved Photoluminescence (TRPL): The samples were excited with a 5-MHz repetition-rate, picosecond-pulse light source at 405 nm, with a beam spot of 10 µm. A Micro Photon Devices single-photon avalanche photodiode (LDHP-670) detector collected the signal, which was filtered by an Acton monochromator (SpectraPro 2300). A time-correlated single photon counting card (Pico Harp TSCPC module and Picosecond Event Timer 300) was used to acquire the signals. Double exponential functions were fitted to extract charge-carrier lifetimes from the resulting decay curves. Temporal resolution was 50 ps.

Thermogravimetric Analysis (TGA): TGA measurements were conducted using TA Q500 instrument. Purified $CsPbBr_3$ NCs were dried under vacuum to obtain a dry powder. In each measurement 5-10 mg of $CsPbBr_3$ NC powder was placed in an alumina crucible, which was placed on a platinum pan. Sample was measured under nitrogen atmosphere with temperature ranges from room temperature to 600 °C at the ramp rate of 10 °C min^{-1}.

Nuclear Magnetic Resonance (NMR) Spectroscopy: Solution ^1H NMR experiments in this study were completed on a Bruker Avance I 9.40 T (ν_0 (^1H) = 400.13 MHz) spectrometer with a Bruker 5 mm BBO probe. A ^1H one-pulse sequence, with a $\pi/2$ pulse length of 10 μs and a recycle delay of 1 s, was employed. Samples were prepared with toluene-d8 solvent and were referenced internally.

All solid state NMR experiments in this study were completed on a Bruker Avance III HD 600 MHz spectrometer with a Bruker 1.9 mm HXY MAS probe. The ^{13}C NMR experiments were completed at 14.1 T (υ_0 (^{13}C) = 150.92 MHz) with an MAS frequency of 12 kHz. A ^{13}C CPMAS pulse sequence, with a contact pulse length of 5000 μs and high power proton decoupling, was employed and resulting data was referenced with respect to adamantane ($C_{10}H_{16(s)}$; δ_{iso} = 38.48, 40.49 ppm). The 2D ^{31}P-^{1}H heteronuclear correlation (HETCOR) NMR experiments were completed at 14.1 T (υ_0 (^{31}P) = 242.97 MHz and υ_0 (^{1}H) = 600.19 MHz) with an MAS frequency of 15 kHz. A ^{31}P-^{1}H CP HETCOR sequence, with a contact pulse length of 5000 μs and high power proton decoupling, was employed and resulting data was referenced with respect to ammonium dihydrogen phosphate ($(NH_4)_2HPO_{4(s)}$; δ_{iso} = 0.99 ppm). A ^{1}H $\pi/2$ pulse length of 2.5 μs, determined on adamantane, and a recycle delay of 2 s were used in all CP experiments.

Fourier Transform Infrared (FTIR) Spectroscopy: Attenuated total reflectance Fourier transform infrared (ATR-FTIR) measurements were performed using a Perkin Elmer Frontier, equipped with a Diamond ZnSe ATR crystal. Spectra were collected from 4000-500 cm-1 (100 scans; 1 cm^{-1} per step).

LED Device Characterisation: LED devices were encapsulated within a glass cavity, sealed with UV-curable epoxy resin, before being withdrawn from the argon-filled glovebox for electroluminescence characterization. A Keithley 2612B was used to obtain the current-voltage characteristics of the LED devices. A scan rate of 1 V s^{-1} (step size 0.1 V, step interval 0.1 s) was used. An integrating sphere (OceanOptics FOIS-1) coupled to a calibrated spectrophotometer (OceanOptics QEPro) was used to capture light emission. An OceanOptics HL-3 Plus vis-NIR light source, calibrated using a procedure and documentation patterned after the ISO 17025, IEC

Guide 115 and JCGM100:2008 (GUM) protocols, is used to calibrate the absolute irradiance measurement of the spectrometer. The edge emission contribution is lost outside the integrating sphere due to placement of LED devices, therefore only forward emission is collected. This method was previously used to measure the external quantum efficiency of organic light emitting diodes.[2,3]

CALCULATIONS

Nanocrystal Concentration:

Nanocrystal solutions were prepared for UV-Visible absorption measurement by diluting 10 µL nanocrystal ink in 3 mL toluene.

The volume fraction (*f*) of the nanocrystals in solution can be calculated from absorbance according to the relation:

$$f = \frac{A}{\mu_i L} \ln(10)$$

From literature, the intrinsic absorption coefficient (μ_i) of $CsPbBr_3$ NCs in toluene at 400 nm = 8.7×10^4. From the UV-Visible absorption spectrum, absorbance (*A*) at 400 nm = 0.275. The path length of the measurement (*L*) = 1 cm.

$$f = \frac{(0.275)}{(8.7 \times 10^4)(1)} \ln(10)$$

$$f = 7.28 \times 10^{-6}$$

The molar concentration (c) can be calculated from the volume fraction according to:

$$c = \frac{f}{N_A a^3 d^3}$$

Where the mean cube edge length (*d*) of the nanocrystals was taken from small-angle x-ray scattering was 10.1 nm, and the lattice constant (*a*) of cubic $CsPbBr_3$ = 0.587 nm.

$$c = \frac{(7.28 \times 10^{-6})}{(6.022 \times 10^{23})(0.587)^3 (10 \times 10^{-9})^3}$$

$$c = 5.98 \times 10^{-5}\ mol\ L^{-1}$$

Thus, the molar concentration of the undiluted nanocrystal ink (c_{ink}) can be calculated:

$$c_{ink} = (5.98 \times 10^{-5}) \times 300$$

$$c_{ink} = 18\ mM$$

Ligand to Nanocrystal Ratio

The maximum photoluminescence intensity was obtained for a molar OPA:$CsPbBr_3$ ratio of approximately 1:1. Thus the number of OPA ligands per nanocrystal is approximately equal to the number of unit cells within each nanocrystal.

$$OPA\ Ligands\ per\ NC = \left(\frac{d^3}{a^3}\right)$$

$$OPA\ Ligands\ per\ NC = \left(\frac{10.1^3}{0.587^3}\right)$$

$$OPA\ Ligands\ per\ NC \approx 5000$$

If we assume that $CsPbBr_3$ nanocrystals are terminated by only CsBr facets, the number of surface bromide sites can be estimated. The density of bromide sites on the surface of $CsPbBr_3$ NCs is equal to the square of the lattice constant for the cubic perovskite structure:

$$a^2 = 0.587^2 = 0.345\ nm^{-2}$$

Dividing the total surface area of the NCs by the surface density of bromide sites:

$$\frac{6 \times (10.1)^2}{0.354} = 1730\ Br^-\ surface\ sites\ per\ nanocrystal$$

Thus, the maximum photoluminescence was obtained when the OPA concentration added introduced a number of ligand in 3 times excess of the maximum number of surface bromide vacancies. However, the concentration at which the PL intensity plateaus (ca. 4 mM) corresponds to around 1000 OPA ligands per nanocrystal.

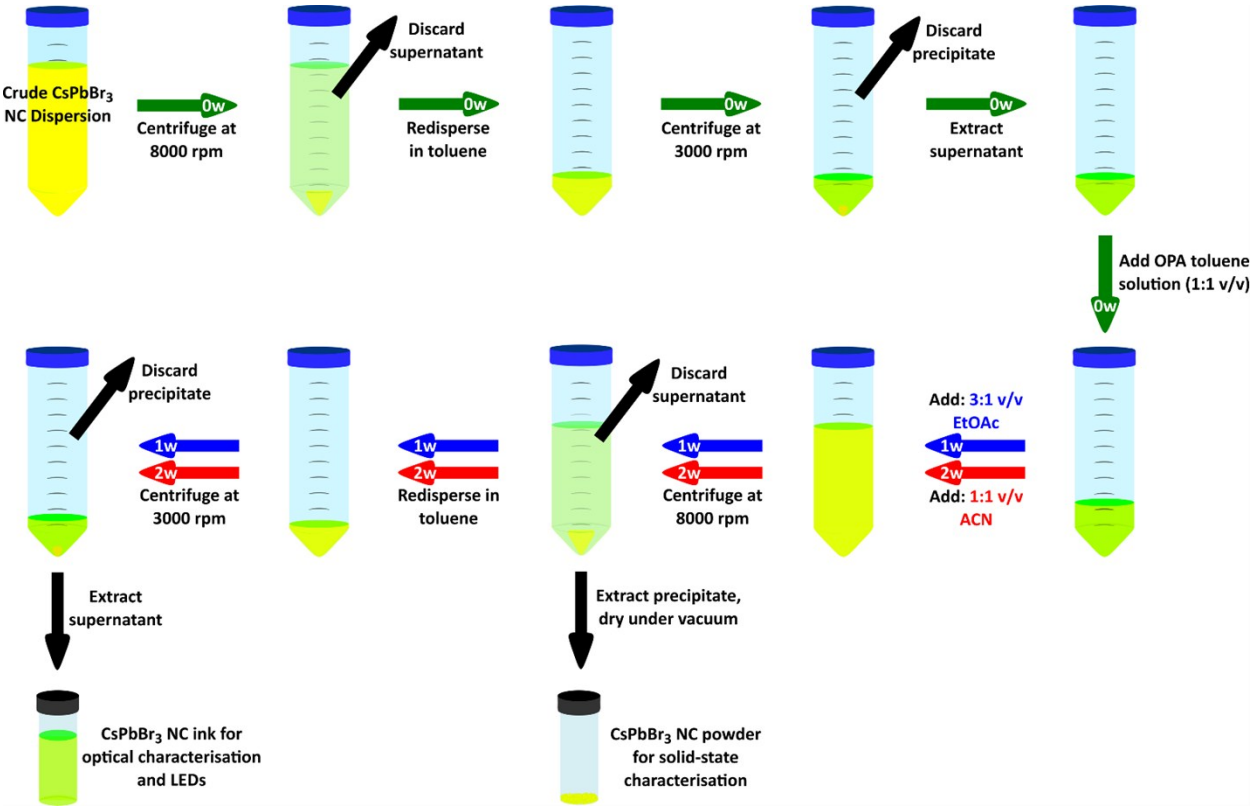

Scheme S1: The purification and ligand exchange protocol employed herein. The green, blue and red arrows represent the NC isolation (0w), 1st purification (1w) and 2nd purification (2w) cycles, respectively. Also shown are the stages of the cycles at which precipitated samples were extracted for solid-state NMR analysis, and NC inks were extracted for optical analysis and LED fabrication.

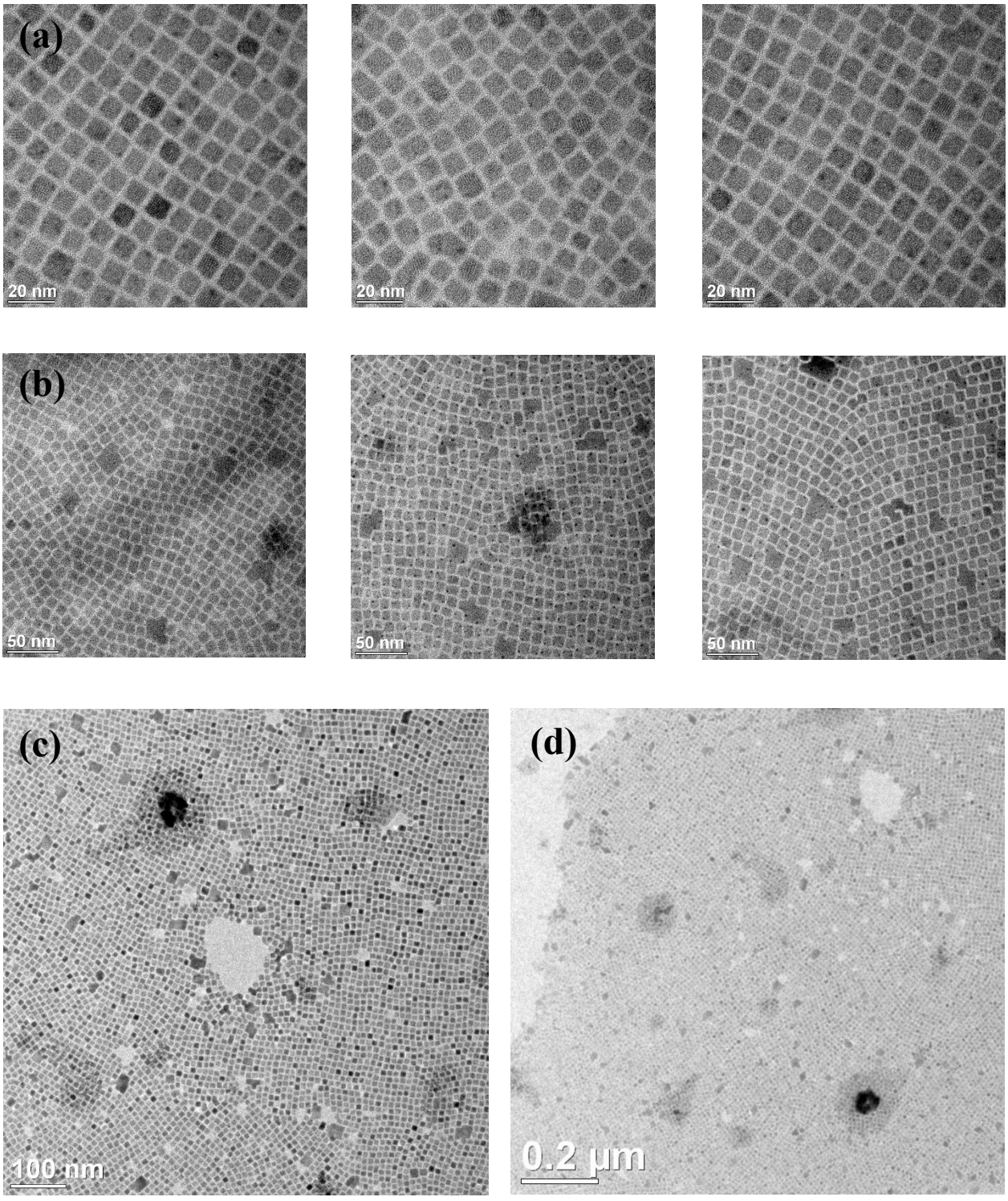

Figure S1: Transmission electron microscopy images of fully-purified OPA-treated $CsPbBr_3$ NCs (OPA−2w). (a)-(d) show images at different magnification.

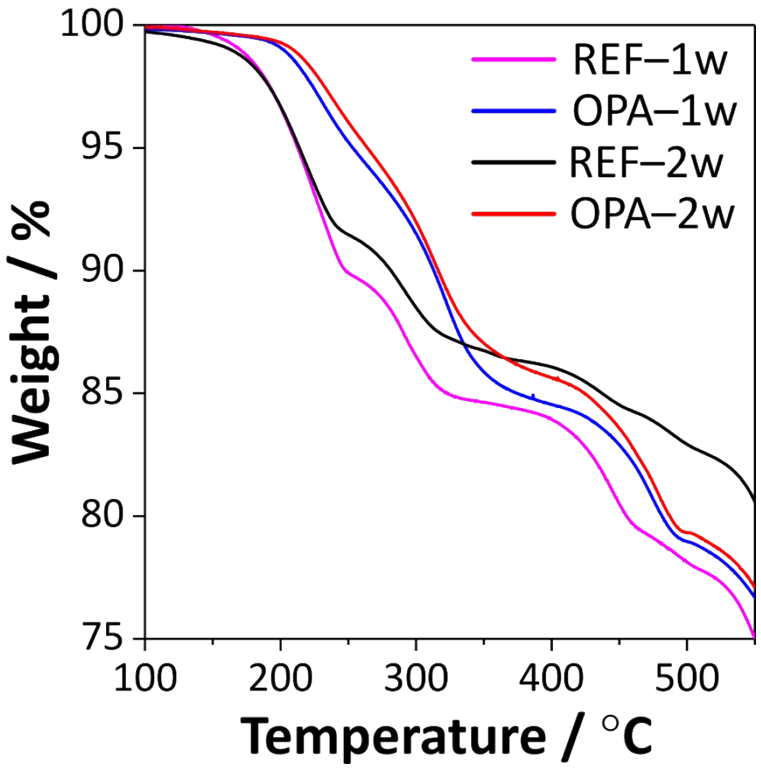

Figure S2: Thermal Gravimetric Analysis, showing the weight loss of each $CsPbBr_3$ NC sample between 100 and 550 °C.

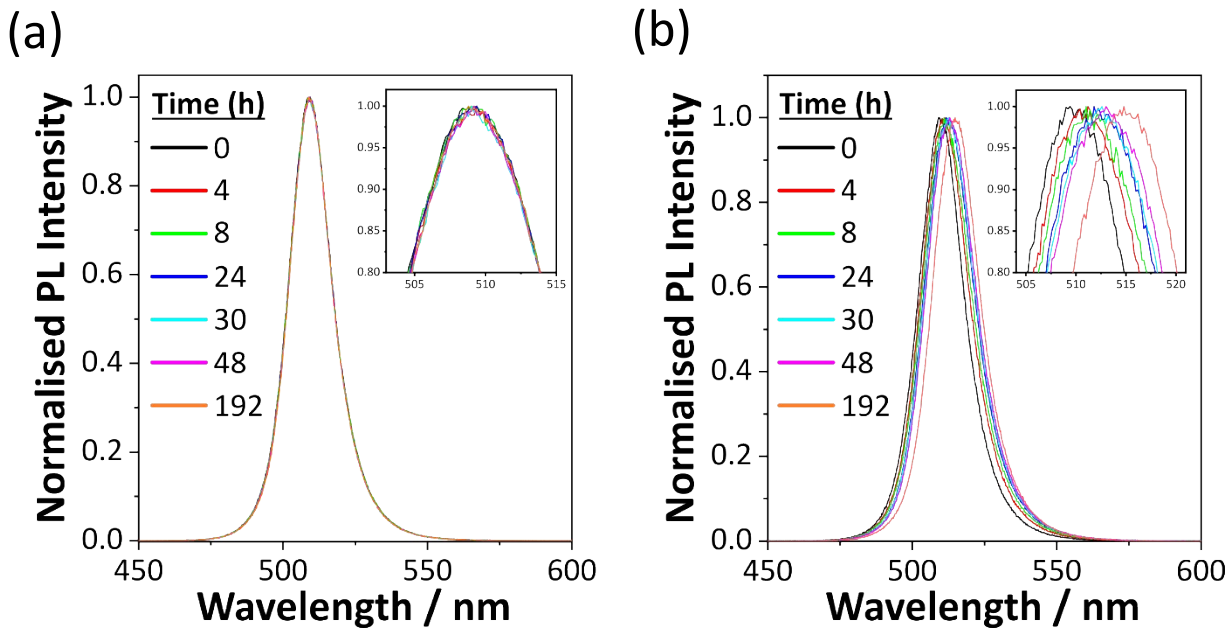

Figure S3: Photoluminescence spectra of (a) OPA−2w and (b) REF−2w $CsPbBr_3$ NC solutions (concentration ≈ 0.05 mg mL^{-1}) monitored over time. Insets show magnified sections of the same spectra at the emission maximum.

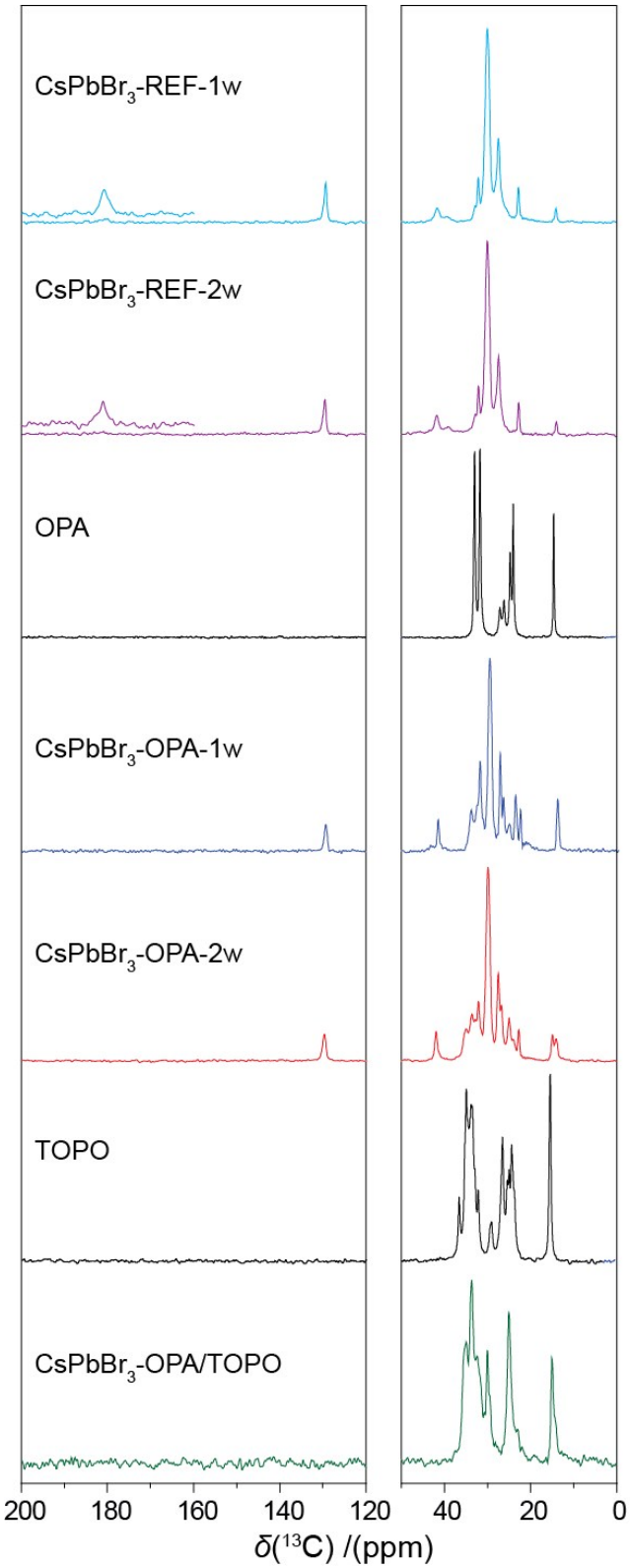

Figure S4: The ^{13}C cross-polarisation magic-angle spinning (CPMAS) NMR spectra of crystalline OPA and TOPO, and each $CsPbBr_3$ NC sample.

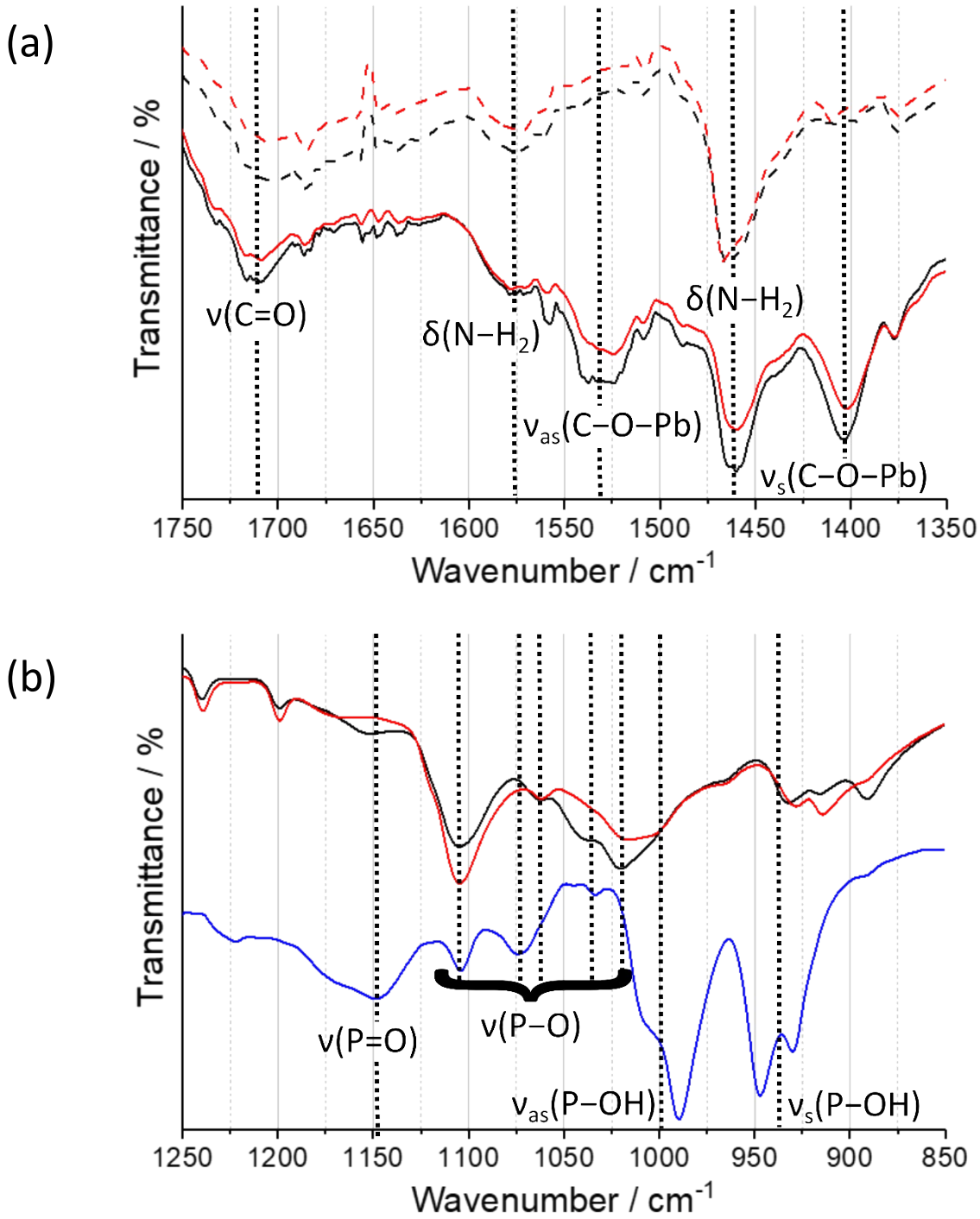

Figure S5: ATR FTIR spectra. (a) REF (solid) and OPA (dashed) NC samples for purified once (black) and twice (red). The C–O stretching region is shown. (b) Crystalline OPA (blue) and OPA NC samples after one purified cycle with 2:1 ethyl acetate (black) and after a second purification cycle with 1:1 acetonitrile (red). The P–O stretching region is shown.[4–7]

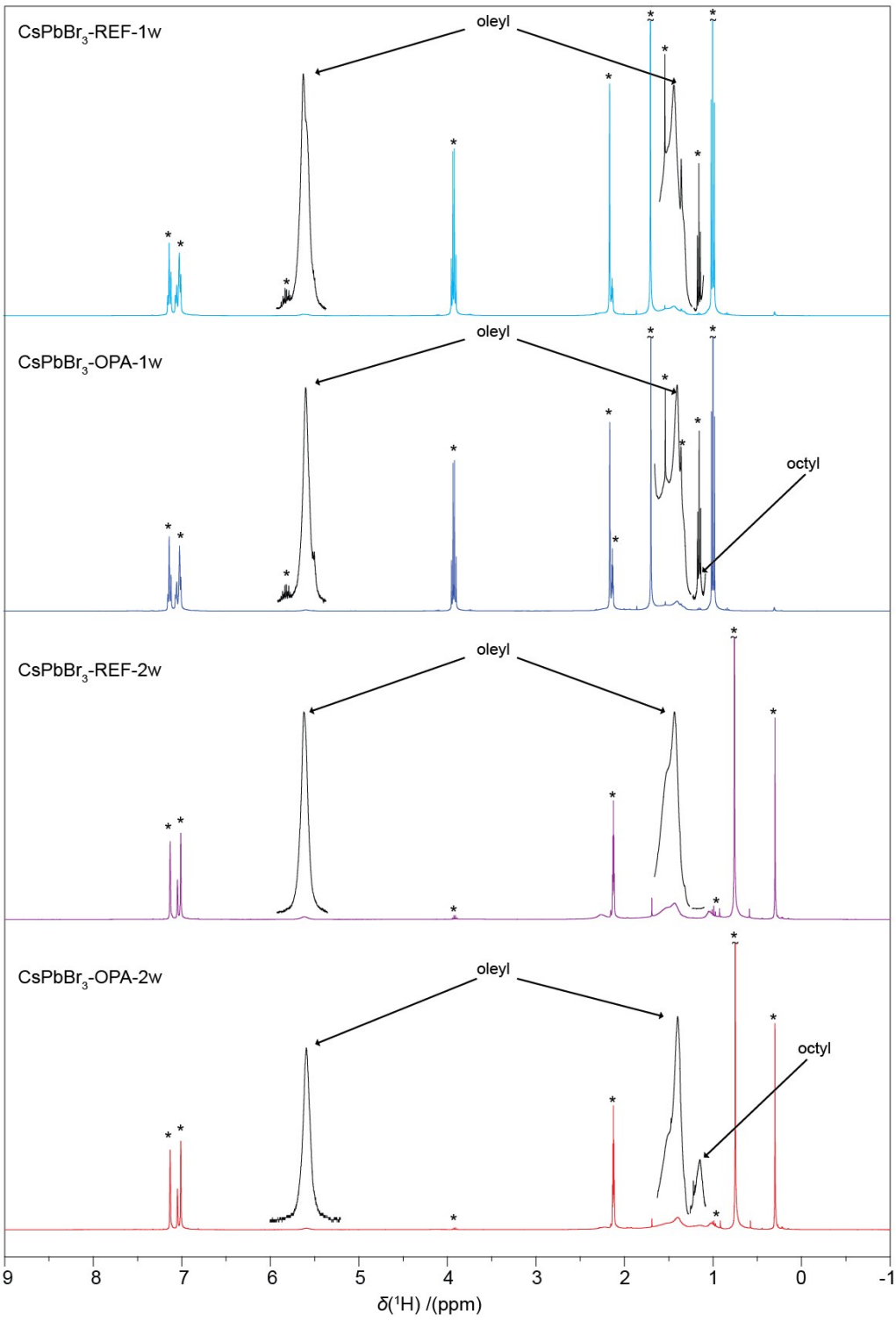

Figure S6: Solution ^{1}H NMR spectra of each $CsPbBr_3$ NC solution. Asterisks (*) denote residual proton signals from the solvent (toluene-d8, toluene) and the antisolvents (ethyl acetate and acetonitrile). Observable broad resonances corresponding to protons in oleyl and octyl chains of the respective bound ligands (OLA/OA and OPA) are labelled.

Table S1: Time-resolved Photoluminescence (TRPL) Data.

	A_1	τ_1 (ns)	A_2	τ_2 / ns	τ_{ave} / ns
REF−2w	0.74	0.78	0.26	3.8	1.54
OPA−1w	0.72	1.07	0.28	6.1	2.48
OPA−2w	0.73	1.44	0.26	10.3	3.77

REFERENCES

1 B. R. Pauw, J. S. Pedersen, S. Tardif, M. Takata and B. B. Iversen, *J. Appl. Crystallogr.*, 2013, **46**, 365–371.

2 Z. Zhang, L. Chen, X. Peng, X. Liang, J. Wang, Y. Niu, X. Dai, H. Cao and Y. Jin, *Nature*, 2014, **515**, 96–99.

3 Y. Cao, I. D. Parker, G. Yu, C. Zhang and A. J. Heeger, *Nature*, 1999, **397**, 414–415.

4 T. Schulmeyer, S. A. Paniagua, P. A. Veneman, S. C. Jones, P. J. Hotchkiss, A. Mudalige, J. E. Pemberton, S. R. Marder and N. R. Armstrong, *J. Mater. Chem.*, 2007, **17**, 4563–4570.

5 L. C. Thomas and R. A. Chittenden, *Spectrochim. Acta*, 1964, **20**, 467–487.

6 L. C. Thomas and R. A. Chittenden, *Spectrochim. Acta*, 1970, **21**, 1905–1914.

7 J. G. Son, E. Choi, Y. Piao, S. W. Han and T. G. Lee, *Nanoscale*, 2016, **8**, 4573–4578.